Mathematical Modeling of a Galvanostatic Soil Electroremediation Process

M. M. Teutli-León
Facultad de Ingeniería, B.U.A.P., Edificio 123, Cd. Universitaria, Puebla, Pue., México, 072570

M. T. Oropeza, I. González, and A. Soria
División de Ciencias Básicas e Ingeniería, UAM-Iztapalapa, Av. San Rafael Atlixco No. 186, Col Vicentina, Iztapalapa, México, D. F.Mexico, 09340

DOI 10.1002/aic.10490
Published online April 11, 2005 in Wiley InterScience (www.interscience.wiley.com).

A mathematical model for galvanostatic soil electroremediation of cadmium-spiked kaolinite was built considering: chemical and electrical properties from both phases, assumption of local equilibrium conditions, electroneutrality from phase interactions, a dynamic surface charge, and surface adsorbed concentrations defined by Boltzmann's equation. Model prediction trends agree with the expected phenomena to occur during an electroremediation process, as far as they show: a right electroosmotic fluid velocity with a suction effect at the anode position, a pH drop at the cathode position, soluble cadmium transport from anode to cathode, as well as cadmium accumulation before reaching the cathode, and a drop in electric potential gradient. Also, model strength allows the prediction of chemical species transient concentration; and provides an insight on species distribution through the spatial domain, while electroremediation takes place. © 2005 American Institute of Chemical Engineers *AIChE J,* 51: 1822–1833, 2005
Keywords: mathematical model, electroremediation, kaolinite, cadmium, chemical speciation

Introduction

Electrokinetic soil remediation has been successfully applied to clayey soils having low heavy metal concentrations. Concern about these metals comes from facts like their high toxicity characteristics,[1] and their solubility by ion exchange process, when the soil saturating solution exhibits an acid pH. [2, 3]

Published soil electroremediation experimental work have considered one of the following approaches: a soil spiked with either one metal[4,5,6,7] or with several metals,[8, 9] as well as successful *in situ* experiments for heavy metal removal.[10, 11] Another type of research has been focused on improving electroremediation process efficiency by either modifying parameters,[12,13,14,15,16,17], or analyzing the interdependency between them.[18,19,20,21,22]

Researchers agree that a main obstacle for process optimization is the time required for each experiment, reported times range from weeks at a laboratory[6,7,8, 13, 14] to months in the field[10, 11]. In order to bypass that limitation, some efforts have been addressed to modeling the process, as it is described in the following paragraphs.

Soil electroremediation mathematical models comprise 1 or 2 spatial dimensions (1-D, and 2-D). Example of the 1-D formulation is the work of Acar et al.,[23] whose model is based on Nernst-Planck's equation, Darcy's law, Ohm's law and some soil physical properties. Other authors have included ionic reactions and an estimation of the electroosmotic flow[24,25,26]; as well as solution electroneutrality plus the zeta-potential concept[27]. On the basis of Acar's theory, a refined model was proposed by Alshawabkeh et al.,[28, 29] in its formu-

Correspondence concerning this article should be addressed to M. M. Teutli-Leon at mteutli@prodigy.net.mx.

lation they consider soil tortuosity as a correcting factor for both electrical conductivity and ion mobility.

In 1995, Jacobs proposed a 2-D electroremediation model[30] based on an electric field applied to a multicomponent system. In this model, He included electroneutrality between phases and some equilibrium relationships for the aqueous phase. Although, none of those relationships account for species transfer between phases.

In 2001, Teutli- León et al.[31] proposed a mathematical model for electroremediation of a cadmium spiked kaolinite; this model is based on a multicomponent system which accounts for soil active sites; also, speciation in the aqueous phase is defined through equilibrium relationships; and transfer of species between phases is approached as an ion exchange process. Even though, model predictions are quite close to the data published by Acar,[7] not all variables exhibit the expected behavior.

In this article, a refinement of the mathematical model formerly published by Teutli- León et al.[31] is proposed. This model formulation considers the following modifications:

1. Redefinition of boundary conditions, in order to achieve consistency between the specified conditions for the whole set of variables.

2. Inclusion of a soluble nitrate ion, as an additional anionic species in the aqueous phase. Since experimental reports[7,8] refer synthetic samples were prepared by dissolution of either a nitrate or a sulfate salt.

3. Redefinition of aqueous surface concentrations, as it is considered by Boltzmann's distribution.[32] This relationship defines the surface concentration in terms of the bulk aqueous concentration corrected by the electrical potential at the soil surface.

$$c_i = c_{i0}\exp\{-ze(\Psi - \Psi_0)/kT\}$$

Considering that an electroremediation process results from an interactive process between electrodes, soil and saturating solution; then, any observed response should be the result of the physical, chemical and electrical properties from both phases. Since electrode transfer kinetics is fast, by including the proposed modifications it is expected that model predictions satisfy the observed experimental behavior during an electroremediation process.

Model Formulation

On the basis of experimental issues, a mathematical model capable of simulating the electroremediation process, should be based on the following concepts:

1. *Electroremediation takes place in a two phase system*. In a reference element volume, a fraction is occupied by the solid phase; and voids between particles are filled by the fluid phase. Also, soil is considered a fixed phase, while the saturating fluid is taken as a moving phase.

2. *Soil ion exchange capacity is defined by the amount of soil active sites*. In clayey soils ion exchange capacity is highly dependent on soluble ion concentrations,[33, 34] and these concentrations are changing because of both electrode reactions and transport processes.

3. *Chemical speciation takes place in both phases*. At the aqueous phase, ions can be either free or complexed with others. At the solid phase, surface adsorbed ions come from either free or complexed soluble ions.[35] At this stage, only complexation and precipitation reactions are allowed, in such a way that the oxidation numbers are not altered during the course of reactions.

4. *A mass balance for a component i should be performed on a reference volume element*. Total ion concentration must be the summation of ion concentrations in both aqueous and solid phases. A chemical species is referred to as component *i*. Time variations for *i* in the reference volume element, are defined by the aqueous phase flux, and the chemical reactions taking place in both phases.[36]

5. *Aqueous phase flux takes place from anode to cathode*. Aqueous flux is a consequence of the existence of concentration, hydraulic and electric gradients; these gradients induce occurrence of diffusion, convection and migration processes. According to Jacobs,[30] migration process is the fastest one; also, the electric field imposes a preferential path (from anode to cathode) for transport to occur.

6. *The total electrical resistance is the summation of resistances from each phase*. Soil resistance is defined as the reciprocal of the soil conductance, while aqueous phase resistance is determined not only by aqueous ionic content, but also by convective and diffusive processes taking place inside it.[37]

7. *The hydraulic gradient enhances fluid displacement through the soil*. For clayey soils undergoing electroremediation, the hydraulic gradient in the system is defined by two main contributions: soil ion content and the applied electric field.[38]

8. *The observed fluid velocity is proportional to the surface processes and intensity of the disturbing forces*. These disturbing forces are provided by both hydraulic and electric gradients.[39]

9. *Electroneutrality in the reference volume element is established from phase interactions*. Any noncompensated electric charge in either solid or aqueous phase must be of the same magnitude and opposite sign than that in the other phase.[39]

Mass balances in the aqueous phase

The earlier nine statements are the basis for developing all model equations. The model formulation starts with the governing equations reported by Bird et al.[40]. In an aqueous system, a transient mass balance for a component or chemical species *i* is expressed as

$$\frac{\partial c_i}{\partial t} = -\nabla \cdot \mathbf{N}_i + R_i \tag{1}$$

In electrochemical processes the electric field provides the main force for ions movement[41]; then, $\mathbf{N}_i$ must be defined by the Nernst-Planck equation[41], which accounts for diffusive, convective and migration contributions

$$\mathbf{N}_i = -D_i\nabla c_i - z_i\frac{F}{RT}D_i c_i \nabla\Psi + c_i\mathbf{v} \tag{2}$$

Considering a complete set of ionic species which remains unaffected by chemical reactions, and denoting each one by an

α subindex, where $\alpha = 1,\ldots,n$, transient mass balances can be formulated as

$$\frac{\partial c_\alpha}{\partial t} = -\nabla \cdot \mathbf{N}_\alpha \quad \alpha = 1, \ldots, n \tag{3}$$

Where

$$c_\alpha = c_{\alpha 0} + \chi_\alpha \tag{4}$$

Being $c_{\alpha\ 0}$ free α, and χ_α represents complexed α, which is calculated as follows

$$\chi_\alpha = \sum_{i=1}^{na} Ke_i a_i \prod_k B^{a_{ik}} \tag{5}$$

Some of the required soluble chemical equilibrium constants (Ke) are reported in the literature[42, 43]. Also the corresponding Nernst-Planck equation for α is expressed as

$$\mathbf{N}_\alpha = -D_\alpha \nabla c_\alpha - z_\alpha \frac{F}{RT} D_\alpha c_\alpha \nabla \Psi + c_\alpha \mathbf{v} \tag{6}$$

Where, D_α is a function of the binary diffusion coefficients for each α ionic species. Considering that any α ionic species is included within the c_i chemical species; then, the α-total concentration is the summation for all chemical species containing the α ion

$$c_\alpha = \sum_{i=1}^{na} \nu_{\alpha i} c_i \tag{7}$$

In Eq. 7 $\nu_{\alpha i}$ represents the stoichiometric number of α ions in the molecule of the i-th chemical species. If Eq. 1 is multiplied times $\nu_{\alpha i}$, the summation for all chemical species defines the transient mass balance for c_α; by doing so, the following equation is obtained

$$\frac{\partial}{\partial t} \sum_{i=1}^{n} \nu_{\alpha i} c_i = -\nabla \cdot \left[\sum_{i=1}^{n} \nu_{\alpha i} \mathbf{N}_i \right] + \sum \nu_{\alpha i} R_i \tag{8}$$

For α ionic species, the last term in Eq. 8 is equivalent to the source-sink rate due to chemical reactions R_α. However, conservation of ionic species requires $R_\alpha = 0$, this condition follows from the fact that redox reactions have not been considered, and it allows Eq. 8 to become an equivalent expression to Eq. 3. The flux term requires multiplying Eq. 2 times $\nu_{\alpha i}$, the resulting equation can be compared with Eq. 6 to establish the following identities:

$$D_\alpha \nabla c_\alpha = \sum_{i=1}^{n} D_i \nabla (\nu_{\alpha i} c_i) \tag{9}$$

$$\frac{F}{RT} z_\alpha D_\alpha c_\alpha \nabla \Psi = \frac{F}{RT} \sum z_i D_i \nu_{\alpha i} c_i \nabla \Psi \tag{10}$$

$$c_\alpha \mathbf{v} = \left[\sum_{i=1}^{n} \nu_{\alpha i} c_i \right] \mathbf{v} \tag{11}$$

in terms of the total α ionic species. The full expression for Eq. 8, after considering D_α as a constant becomes

$$\frac{\partial c_\alpha}{\partial t} = D_\alpha \nabla^2 c_\alpha + \frac{F}{RT} z_\alpha D_\alpha \nabla \cdot (c_\alpha \nabla \Psi) - \nabla \cdot (c_\alpha \mathbf{v}) \tag{12}$$

Mass balance in the two-phase system

In a two-phase system such as a water saturated soil, transient mass balances should involve interactions between both phases. The solid phase provides some ionic species to the liquid in such a way that ionic mass balances in the liquid, given by Eq. 3, can be reformulated as follows

$$\frac{\partial c_\alpha}{\partial t} = -\nabla \cdot \mathbf{N}_\alpha + \frac{1-\theta}{\theta} R_{s\alpha} \tag{13}$$

The last term includes the symbol θ which represents the void fraction in the soil, which is occupied by the liquid phase. Also, $R_{s\alpha}$ corresponds to the generation rate of α ionic species at the solid matrix. This term accounts for the amount of α being transferred from the solid to the liquid phase by unit of liquid volume.

On the other hand, the solid phase concentration is modified as consequence of surface reactions

$$\frac{\partial c_{s\alpha}}{\partial t} = -R_{s\alpha} \tag{14}$$

In which $c_{s\alpha}$ is the α concentration in the solid phase. In order to define the $c_{s\alpha}$ concentration, soil surface sites (Sj^-) are considered to have a single-valence charge, so any free or complexed soluble species (c_i) can interact with one or more soil sites; also, it is possible that a soluble complex, with a residual charge, might be adsorbed onto soil sites. So far, the α total concentration onto the solid phase, similarly to Eq. 5, is given by

$$c_{s\alpha} = \sum \nu_{\alpha i} Kd_i c_i^{a_i} Sj^{b_i} \tag{15}$$

In this equation Kd_i is the i^{th} ion exchange equilibrium constant for a surface process; a_i corresponds to the number of soluble species interacting with b_i soil sites to form the i^{th} surface complex.

The net movement of the α species into a representative volume element must be a consequence of all processes taking place in both phases. In order to couple mass balances from both phases, concentrations should be referred in mol cm^{-3}_{Total}. This change in reference should require Eq. 13 being multiplied times the aqueous phase volume fraction and Eq. 14 times the solid fraction, resulting in

$$\frac{\partial}{\partial t}(\theta c_\alpha) = -\nabla\cdot(\theta \mathbf{N}_\alpha) + (1-\theta)R_{s\alpha} \tag{16}$$

$$\frac{\partial}{\partial t}[(1-\theta)c_{s\alpha}] = -(1-\theta)R_{s\alpha} \tag{17}$$

By adding Eqs 16 and 17 an expression for the transient total mass balance is obtained

$$\frac{\partial}{\partial t}[\theta c_\alpha + (1-\theta)c_{s\alpha}] = -\nabla\cdot(\theta \mathbf{N}_\alpha) \tag{18}$$

Nernst-Planck Eq. 2 involves fluid velocity $\mathbf{v}$ and electric potential Ψ as variables. The procedure to obtain the corresponding equations is described in the following paragraphs.

Fluid velocity and electric potential defined in a two-phase system

Verbrugge reported a model for ion exchange membrane processes[39]; in this, he included a modified form of Schlög's equation for transport in porous media. This equation describes fluid velocity in terms of two disturbing forces: an electric field and a hydrostatic pressure. The proposed equation is

$$\mathbf{v} = \frac{k_{sm}}{\eta}\left[\left(z_m c_m + \sum_{i=1}^{n} z_i c_{si}\right)F\nabla\Psi - \nabla P\right] \tag{19}$$

Considering that a water saturated clay behaves like a membrane[33, 38, 44]; there is a similarity between membrane active sites (c_m) and soil active sites (Sj). Equation 19 can be used to describe the electroosmotic fluid velocity in a saturated soil. The membrane adsorbed species (c_{si}) would correspond to the soil surface adsorbed species ($c_{s\alpha,i}$) which accounts for adsorption onto protonated sites, as well as possible interactions of surface sites with soluble species in which a residual charge is produced, so far the membrane sites charge (z_m) should correspond to soil sites charge (z_{Sj}). Then, electro osmotic fluid velocity can be estimated from the following equation

$$\mathbf{v} = -\frac{k_s}{\eta}\left[\left(z_{Sj}Sj + \sum_{i=1}^{n} z_i c_{s\alpha,s}\right)F\nabla\Psi - \nabla P\right] \tag{20}$$

Here, k_s corresponds to the hydraulic soil conductivity, and pressure (P) is a new variable, thus an additional equation is required in order to obtain a closed equation set.

In porous media theory applied to saturated soils, the velocity field of an incompressible fluid is solenoidal[39]

$$\nabla\cdot\mathbf{v} = 0 \tag{21}$$

By applying this criteria to Eq. 20, an additional equation involving the pressure is obtained

$$\left(z_{Sj}Sj + \sum_{i=1}^{n} z_i c_{s\alpha,i}\right)F\nabla^2\Psi + \left(\sum_{i=1}^{n} z_i\nabla c_{s\alpha,i}\right)\cdot F\nabla\Psi - \nabla^2 P = 0 \tag{22}$$

The behavior of electric potential is based on Newman's dilute solutions theory,[41] in this electric current density is defined in terms of ionic fluxes for a binary electrolyte, as follows

$$\mathbf{I} = F\sum_{i=1}^{n} z_i\mathbf{N}_i \tag{23}$$

By replacing the flux terms, an equation to calculate the electric potential gradient (Ψ) is obtained

$$\nabla\Psi = -\frac{\mathbf{I}}{\mathrm{K}} - \frac{F}{\mathrm{K}}\left(\sum_{i=1}^{n} z_i D_i\nabla c_i\right) + \frac{F}{\mathrm{K}}\left(\sum_{i=1}^{n} z_i c_i\right)\mathbf{v} \tag{24}$$

So far, aqueous ion content defines the ionic solution conductivity K as follows:

$$\mathbf{K} = \frac{F^2}{RT}\sum_{i=1}^{n} z_i^2 D_i c_i \tag{24a}$$

Newman's theory for porous electrodes (a two-phase system) establishes that total current density is a solenoidal vector field, as a consequence of the assumed reference volume element electroneutrality. This is expressed as

$$\nabla\cdot\mathbf{I}_{\text{solid}} + \nabla\cdot\mathbf{I}_{\text{aqueous}} = 0 \tag{25}$$

Relationship between current density and potential gradient for each phase is based on Ohm's law, with constant electrical conductivities:

$$\mathbf{I}_{\text{solid}} = -\Gamma\nabla\Psi_{\text{solid}} \tag{26}$$

Where Γ is the solid phase electrical conductivity; and

$$\mathbf{I}_{\text{aqueous}} = -K\nabla\Psi_{\text{aqueous}} \tag{27}$$

Ψ_{aqueous} can be obtained by Eq. 24; and the total potential gradient in a clay-water system results from adding the contributions of both solid and aqueous phases.[37, 41] The resulting equation is:

$$\nabla\Psi = -\frac{\mathbf{I}}{\Gamma} - \frac{\mathbf{I}}{K}\left(\sum_{i=1}^{n} z_{\alpha i}D_{\alpha i}\nabla c_{\alpha i}\right) + \frac{F}{\mathrm{K}}\left(\sum z_{\alpha i}c_{\alpha i}\right)\mathbf{v} \tag{28}$$

Finally, electroneutrality in the reference elementary volume means that at any time, charges on the soil surface are compensated by those in the fluid phase. In Verbrugge's membrane model[39] electroneutrality is expressed as follows:

$$z_m c_m + \sum_{i=1}^{n} z_i c_{i,\text{ads}} + \sum_{i=1}^{n} z_i c_i = 0 \tag{29}$$

This expression cannot be applied directly to this model. As it was done for velocity, from Eq 19 to Eq. 20; Eq. 29 should be modified to express the electroneutrality in a total (two-phase) volume reference for a water saturated clay. In this way, the equation for soil active sites (Sj^-) was obtained

$$(1-\theta)\left[z_{SJ}S_J + \sum_{i=1}^{n} z_{\alpha i}c_{s\alpha,i}\right] + \theta \sum_{i=1}^{n} z_{\alpha i}c_{\alpha i} = 0 \tag{30}$$

The equations proposed in previous paragraphs are used to model the electroremediation of a cadmium spiked kaolinite. System description accounts for soluble species being transported through the soil by the action of the electric field; also a dynamic interaction between soluble and adsorbed species is considered. The resulting model considers Eq. 18 to describe the transport of four basic soluble ions (H^+, OH^-, Cd^{+2}, NO_3^-); Eq. 20 for velocity (**v**), Eq. 22 for pressure (P), Eq. 28 for electric potential (Ψ); and Eq. 30 for active soil sites (Sj^-). Electrode separation (L) is used as a characteristic length of the space variable (X), considering 0 as the anode position, and L as the cathode position. Initial (IC) and boundary conditions (BC) for each variable, are defined by the following equations

$$\mathrm{H}^+ = \begin{cases} I.C.\ (t=0) & [H^+]^0 = 10^{-pH_0} \\ B.C.1.\ (X=0) & v^0[\mathrm{H}^+]^0 + \dfrac{I}{nF} = \mathbf{N}_{\mathrm{H}^+} \\ B.C.2.\ (X=L) & [\mathrm{H}^+][\mathrm{OH}^-] = \mathrm{K}_w \end{cases} \qquad 0 \le X \le L \tag{31}$$

$$\mathrm{OH}^- = \begin{cases} I.C.\ (t=0) & [\mathrm{OH}^-]^0 = \dfrac{\mathrm{K}w}{[\mathrm{H}^+]^0} \\ B.C.1.\ (X=0) & [\mathrm{H}^+][\mathrm{OH}^-] = \mathrm{K}w \\ B.C.2.\ (X=L) & \dfrac{I}{nF} = -\mathbf{N}_{\mathrm{OH}^-} \end{cases} \qquad 0 \le X \le L \tag{32}$$

$$\mathrm{Cd}^{+2} = \begin{cases} I.C.\ (t=0) & [\mathrm{Cd}^{+2}] = [Cd^{+2}]_{\text{ads}} \\ B.C.1.\ (X=0) & [\mathrm{Cd}^{+2}] = 0 \\ B.C.2.\ (X=L) & \nabla[\mathrm{Cd}^{+2}] = 0 \end{cases} \qquad 0 \le X \le L \tag{33}$$

$$\mathrm{NO}_3^{-1} = \begin{cases} I.C.\ (t=0) & [\mathrm{NO}_3^-] = [\mathrm{NO}_3^-]^0 \\ B.C.1.\ (X=0) & \nabla[\mathrm{NO}_3^-] = 0 \\ B.C.2.\ (X=L) & [\mathrm{NO}_3^-] = 0 \end{cases} \qquad 0 \le X \le L \tag{34}$$

$$\Psi = \{B.C.1.\ (X=0) \quad \Psi = 0 \tag{35}$$

Table 1. Experimental Conditions*

	Parameter	Value
1.	Cylindrical system:	
	radius	5.1 cm
	length	10.2 cm
2.	Applied current density	3.7×10^{-5} A cm^{-2}
3.	Cadmium initial concentration	105×10^{-6} g Cd g kaolinite^{-1}
4.	Porosity	0.62
5.	Initial pH	4.4
6.	Kaolinite mass	1 Kg
7.	Solution of 100 mg L^{-1} de $Cd(NO_3)_2$	1.5 l
8.	Observed potential gradient	2.5–4.5 V cm^{-1}
9.	Electroosmotic permeability	1×10^{-4}–1×10^{-6} cm^2 V^{-1} s^{-1}
10.	Experimental time	39.9 d

Acar et al[7]

$$P = \begin{cases} B.C.1.\ (X=0) & P = P^0 \\ B.C.2.\ (X=L) & \nabla P = \dfrac{P_{x=L} - P_{x=0}}{L} \end{cases} \tag{36}$$

Initial free soluble ion concentrations are indicated by [ ]°.

Because there are no reports about specific ion exchange equilibrium constants for kaolinite surface sites (Sj^-); it was assumed that any reactive site corresponds to either a silanol (SiO^-) or an aluminol (AlO^-),[45] and supported by a central valence/coordination number ratio of 4/4 for a silanol group and 3/6 for an aluminol group, then probability of forming a site on a silanol group is twice that on aluminol.[46] Also, surface chemical reactions are defined following Huang's approach.[34] A detailed description of chemical reactions and the corresponding equilibrium constants, included in model formulation, are cited in Appendix A.

Numerical implementation of the proposed mathematical model was done based on the following approach:

1. The characteristic times reported by Jacobs[30] show that migration is the fastest transport process; therefore, main transport takes place from anode to cathode. This consideration allowed restricting space dimensions to 1-D.

2. Time derivatives are expanded in a forward finite differences scheme.

3. Space derivatives are expanded in polynomial expressions by using the orthogonal collocation method. This method, in the finite element option,[47] allowed to approach the highly nonlinear concentration profiles observed during electroremediation experiments.

4. The solution algorithm was built using digital visual FORTRAN; plus the NEQBF subroutine for nonlinear equations from IMSL library, and finite element orthogonal collocation subroutines reported by Finlayson.[47]

Model Predictions

Validation of model predictions was done by using experimental data reported by Acar et al.,[7] and listed in Table 1. It is important to remark that the number of predicted points do not match the number of experimental ones, because model equations form a highly nonlinear system, and after several trial runs, it was observed that an stable performance was obtained by dividing the spatial domain in two segments with one

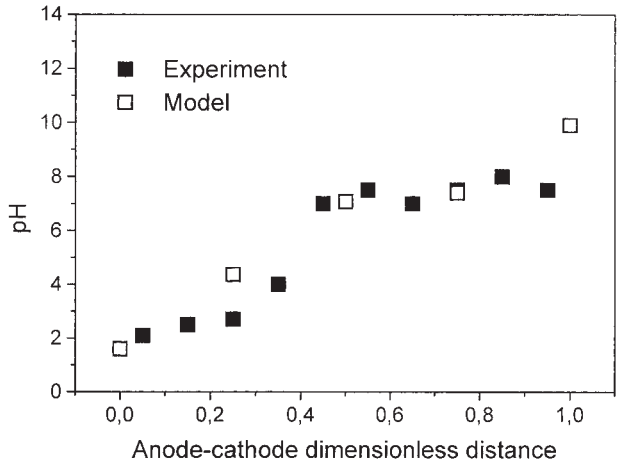

Figure 1. Predicted pH vs. data from experiment CD03 reported by Acar [7], in which a cadmium spiked kaolinite was electroremediated during 39 days.

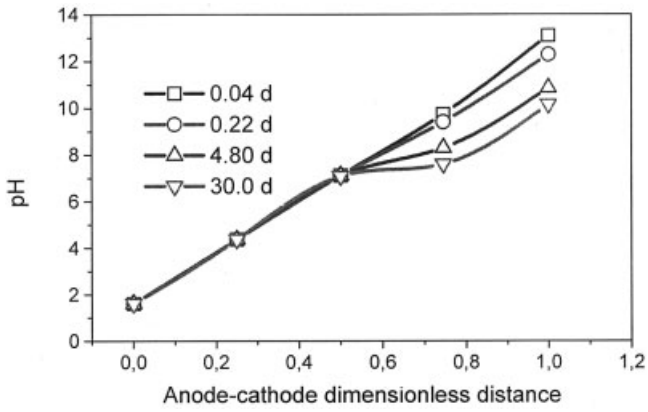

Figure 3. Evolution of proton (pH) profiles simulated for electrode gap = 10.2 cm; I = 0.037 mA cm^{-2}; $Cd_0 = 1.05 \times 10^{-4}$ g Cd(g kaolinite) $^{-1}$; porosity = 0.6; $pH_0 = 4.4$; hydraulic permeability = 1×10^{-6} cm s^{-1}.

internal point, which produces a total of three internal points plus the two boundaries. This selection allowed to get predictions for longer time periods.

In Figures 1 and 2 model predictions (open squares) are compared with experimental pH and residual cadmium (solid squares). It can be observed that predicted values do not match the experimental ones; although their trend is quite close to the experimental one.

Once the comparison between predictions and experimental values showed an acceptable approach, it was convenient to analyze how each one of the variables fits to the expected behavior in an electroremediation process.

During the electroremediation process it is expected that the acid front penetrates into the soil and reaches the cathode position; as a consequence, the pH at the cathode position gets lower values as the process takes place. In Figure 3, pH profiles are shown at four advancing times, with the same initial conditions. It can be observed that proton concentration $[H^+]$ accomplished the expected behavior, which implies a higher concentration close to the anode, and a lower one in the cathodic region (0.5–1.0). At the anodic region (0–0.3) protons exhibit a quasi-stable concentration, which is a consequence of two simultaneous processes taking place at the anode: a constant rate of protons production and a suction effect by the fluid velocity.

Metal solubilization is a consequence of high proton concentration, which increases ion exchange interactions between solid and aqueous phase. Soluble metals migrate to the cathode interacting with the alkaline front through reactions such as neutralization, complexation and precipitation; these interactions drive the maximum metal concentration to occur before reaching the cathode. In Figure 4 concentration profiles for free soluble cadmium are shown. It can be observed that cadmium tendency satisfies expected experimental trends: soluble cadmium concentration is increased by an ion exchange process;

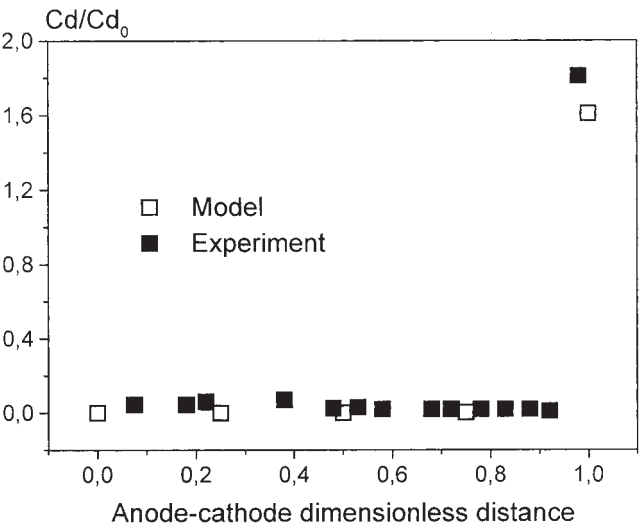

Figure 2. Predicted total cadmium versus experimental residual cadmium data from experiment CD03 reported by Acar[7].

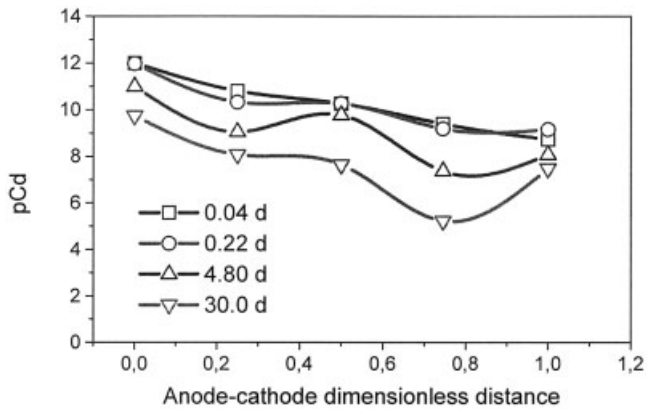

Figure 4. Evolution of free cadmium (pCd) profiles simulated at the electrode gap = 10.2 cm; I = 0.037 mA cm^{-2}; $Cd_0 = 1.05 \times 10^{-4}$ g Cd(g kaolinite) $^{-1}$; porosity = 0.6; $pH_0 = 4.4$; hydraulic permeability = 1×10^{-6} cm s^{-1}.

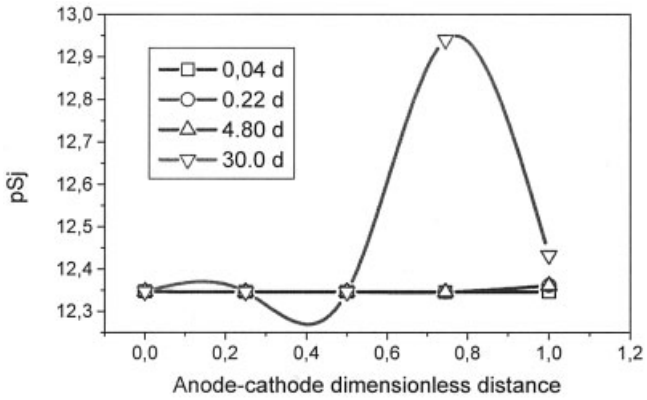

Figure 5. Evolution of soil active sites (pSj) profiles simulated electrode gap = 10.2 cm; I = 0.037 mA cm^{-2}; $Cd_0 = 1.05 \times 10^{-4}$ g Cd(g kaolinite) $^{-1}$; porosity = 0.6; $pH_0 = 4.4$; hydraulic permeability = 1×10^{-6} cm s^{-1}.

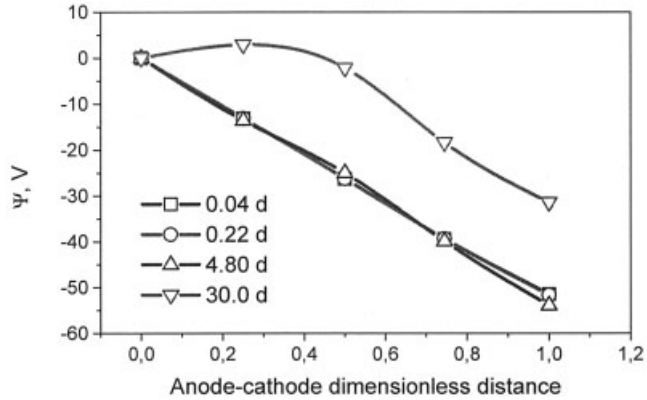

Figure 6. Evolution of electric potential (Ψ) profiles simulated for: electrode gap = 10.2 cm; I = 0.037 mA cm^{-2}; $Cd_0 = 1.05 \times 10^{-4}$ g Cd(g kaolinite)$^{-1}$; porosity = 0.6; $pH_0 = 4.4$; hydraulic permeability = 1×10^{-6} cm s^{-1}.

but it is lowered by the electroosmotic flow which induces cadmium movement from anode to cathode. Also, predictions show that soluble cadmium concentration at the cathode is smaller than that at the previous position.

Active soil sites are sensitive to pH variations in the aqueous phase, and it is expected that protonation (SjH_2^+) takes place at acid pH, while deprotonation (Sj^-) occurs at alkaline pH. Concentration profile predictions for active sites, as a function of advancing times are shown in Figure 5; it can be observed that a higher response is exhibited at the cathodic region (0.5–1.0). And even though maximum variation is about 0.6 orders of magnitude, it is obvious that soil sites concentration exhibit a dynamic response as electroremediation takes place. The minimal variation in respect to other variables, seems to be a consequence of two factors: (a) the small value of the involved ion exchange equilibrium constants; and (b) the inclusion of the electric potential to correct soluble concentration in surface reactions definition; since the electric potential is a strong driving force that could induce accumulation of chemical species at the interface, then the occupancy of active sites should be increased.

Electric potential gradient is highly dependent on the medium electrical conductivity which, for a two-phase system, must be the summation of the conductivities from both phases. In the proposed model formulation, it is assumed that soil conductivity remains constant during electroremediation; but that is not the case for the fluid conductivity, which is modified as the acid and the alkaline front penetrates into the soil. Predictions for electric potential are shown in Figure 6, a linear gradient is shown at short times; but for long times predictions exhibit a composite profile with at least two regions: one of lower gradient in the anodic region; and other with a higher gradient at the cathodic region. In these profiles the estimated electric potential gradient is about 2.5–4.2 V cm^{-1}, which is close to the values reported by Acar[7].

In an electroremediation process, it is expected that fluid velocity establishes a suction effect at the cathode; therefore its magnitude should be higher at this position. In Figure 7, velocity profiles are shown. It can be observed that a minimum value occurs at the anode position, and this value is several orders of magnitude lower than all other in the domain; and even though velocity at the anodic boundary increases its magnitude, it never comes near the velocity inside the sample. In the middle of the spatial domain, predicted velocity values are nonuniform, but discrepancies between them never exceed one order of magnitude.

It is also expected that alkaline front penetration occurs at a lower rate due to the conjunction of phenomena as the following: (a) hydroxyl ion is migrating in opposite sense to the electroosmotic flow; (b) hydroxyl mobility is smaller than proton mobility, and (c) hydroxyl ion is able to complexing with solubilized metals. Predictions obtained for hydroxyl ions are shown in Figure 8. In this figure, it can be observed that major concentration variations take place at the anodic region, and comparison with pH data, confirms that pOH exhibits lower magnitude variations as the electro remediation process takes place.

The proposed model accounts for 8 variables, the discussion has been done for 6 variables so far, the other two (free nitrate and pressure) have not been discussed because they basically

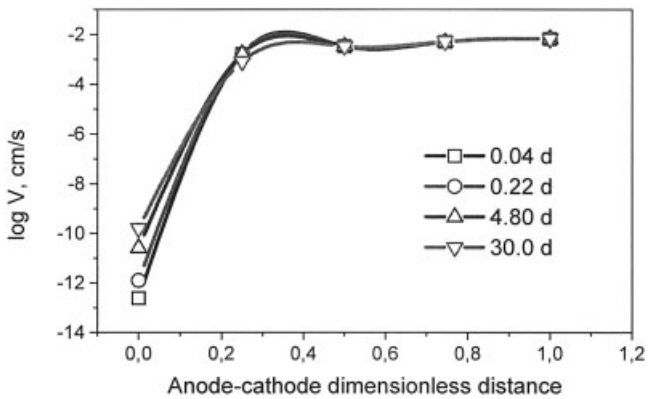

Figure 7. Evolution of velocity (V) profiles simulated for: electrode gap = 10.2 cm; I = 0.037 mA cm^{-2}; $Cd_0 = 1.05 \times 10^{-4}$ g Cd (g kaolinite) $^{-1}$; porosity = 0.6; $pH_0 = 4.4$; hydraulic permeability = 1×10^{-6} cm s^{-1}.

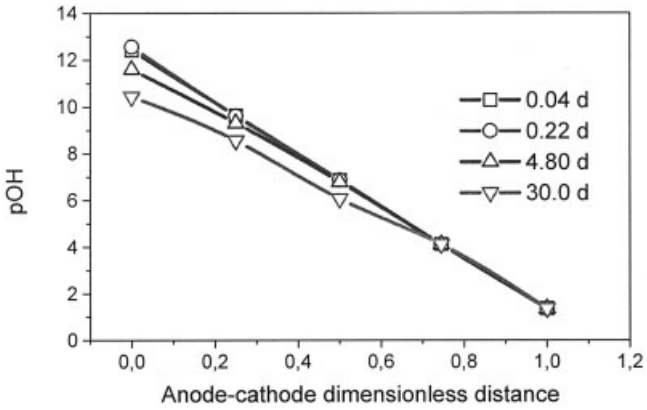

Figure 8. Evolution of hydroxyl (pOH) profiles simulated for: electrode gap = 10.2 cm; I = 0.037 mA cm^{-2}; $Cd_0 = 1.05 \times 10^{-4}$ g Cd(g kaolinite) $^{-1}$; porosity = 0.6; $pH_0 = 4.4$; hydraulic permeability = 1×10^{-6} cm s^{-1}.

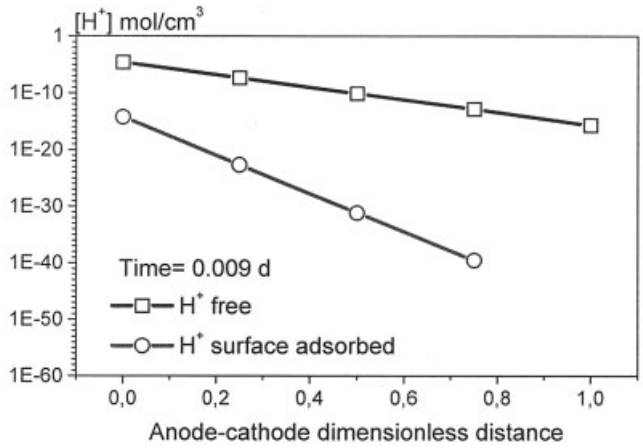

Figure 9. Proton speciation profiles at short time (0.009 d) for an electroremediation of a cadmium spiked kaolinite.

remain constant in all predictions. Although, this fact does not mean that they are not taking part of the whole process. Specifically nitrate in its free form is approximately constant; but its participation becomes relevant in forming soluble complexed and adsorbed species.

Model Predictions for Chemical Species Transient Concentration

On the basis of obtained predictions for ionic species, and the equilibrium relationships included in model formulation, a chemical speciation analysis can be built on the spatial domain. So far, it is possible to follow the response for each one of the chemical species; but in order to minimize the number of lines in each plot, speciation results are lumped in the following groups: free and complexed soluble species, and surface adsorbed species. Also, results shown in this article consider only two sets of predictions: one at short time (0.009 d), and another at long time (50 d).

Transient concentration results are reported as follows: in Figures 9 and 10, proton speciation; in Figures 11 and 12, cadmium speciation; in Figures 13 and 14, hydroxyl speciation; and Figures 15 and 16, for nitrate speciation. For active soil sites speciation results are presented in Figures 17 and 18; in these, data are presented considering free, protonated and surface complexed sites.

Making a correlation between all speciation plots (Figures 9 to 18) the following conclusions can be drawn:

- At the anodic boundary, the magnitude of free soluble ions can be ranged from highest to lowest as follows: protons, nitrate, cadmium and hydroxyl. The last two have similar concentrations, but either one is smaller than nitrate or proton concentration.
- At any time proton adsorption is the main process taking place at the anodic boundary. Also, concentration of adsorbed either nitrate or hydroxyl exhibits a similar order as that of protonated sites; the last one could imply that any protonated site interacts with free anions like nitrate or hydroxyl. Finally, surface adsorbed cadmium concentration is slightly higher than the concentration of surface complexed sites.
- In the region of anodic influence, between 0 and 0.3 of the spatial domain, it is observed that soluble complexed cadmium concentration corresponds to that of nitrate complexes; while calculated hydroxyl soluble complexes concentration is up to 5 orders lower than nitrate complexes concentration. This fact implies that cadmium complexation mainly occurs with nitrate ions.
- Adsorbed nitrate is present in the anodic zone, but its concentration is smaller than any other surface adsorbed species.
- In the middle region, from 0.3 to 0.7 of the spatial domain, adsorbed proton concentration is smaller than surface complexed sites; but the last one is similar to the adsorbed cadmium concentration which implies that surface occupancy is mainly due to cadmium. For adsorbed hydroxyl two regions can be established: one of acidic influence (0.3-0.5) in which hydroxyl concentration is smaller than that of surface complexed sites; and another of alkaline influence (0.5–0.7) in which all three hydroxyl, surface sites and cadmium, have similar concentrations. This implies that either there is a competition between

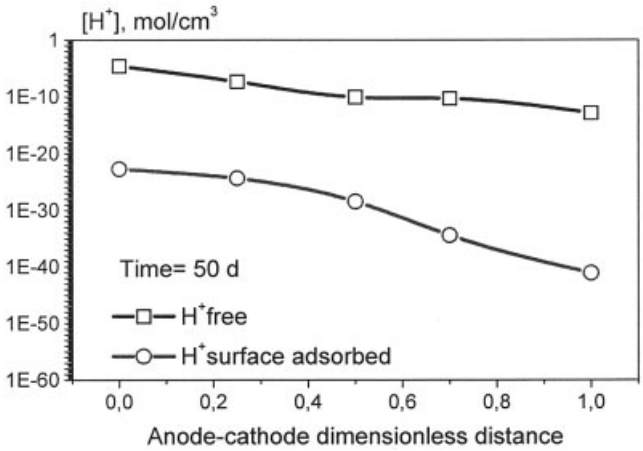

Figure 10. Proton speciation profiles at long time (50 d) for an electroremediation of a cadmium spiked kaolinite.

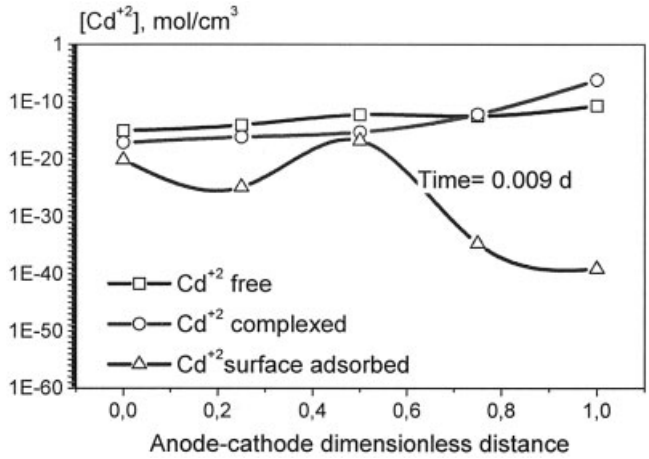

Figure 11. Cadmium speciation profiles at short time (0.009d) for an electroremediation of a cadmium spiked kaolinite.

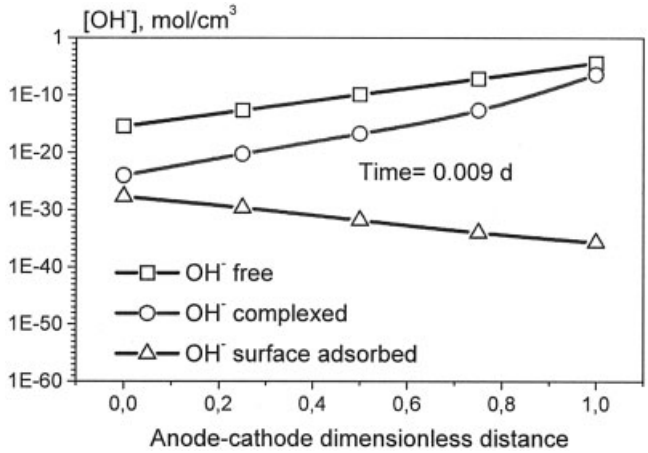

Figure 13. Hydroxyl speciation profiles at short time (0.009 d) for an electroremediation of a cadmium spiked kaolinite.

cadmium and hydroxyl for the surface sites, or complexed cadmium is being retained by soil sites.

- In the middle region, between 0.3 and 0.7 of the spatial domain, free nitrate is the ion of higher concentration. All other free ions (H^{+}, OH^{-}, Cd^{+2}) exhibit similar concentrations.
- In the region near to the cathode, 0.7–1.0 of the spatial domain, it is clear that the concentration of surface complexed sites is similar to that of the adsorbed cadmium concentration. Also, it is obvious that adsorbed hydroxyl plays an important role since its concentration tends to overcome the concentration of surface complexed sites.
- For soluble species in the cathodic region, concentration of free ions can be ranged from highest to lowest, as follows: hydroxyl, nitrate, cadmium and protons. Also it can be observed that concentration of complexed cadmium is similar to that of complexed hydroxyl; and nitrate complexes concentration amounts very small quantities, up to 5 orders less than either hydroxyl or cadmium.

Conclusions

The model developed for an electroremediation process of a cadmium spiked kaolinite successfully simulates the involved kinetics, as far as each of the variables accomplished the expected behavior:

- Proton accumulation with the corresponding pH depletion at the cathode position
- Cadmium desorption and accumulation before reaching the cathode
- A minimal velocity at the anode position, which reaches a maximum at the cathode position, then a suction effect takes place.
- Hydroxyl movement from anode to cathode occurs at a slower rate than proton movement.
- A decrease of the electric potential gradient as pore fluid conductivity increases.

Model formulation based on theories from groundwater, membranes, porous electrodes and soil properties allowed to get an insight on how chemical processes taking place on either phase or between phases, affects the electroremediation of a

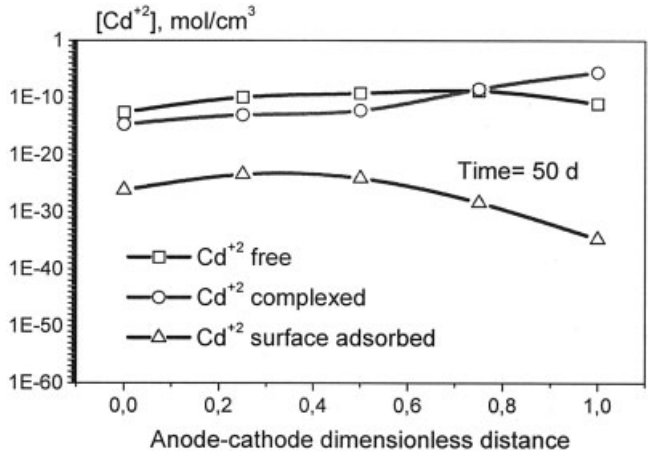

Figure 12. Cadmium speciation profiles at long time (50 d) for an electroremediation of a cadmium spiked kaolinite.

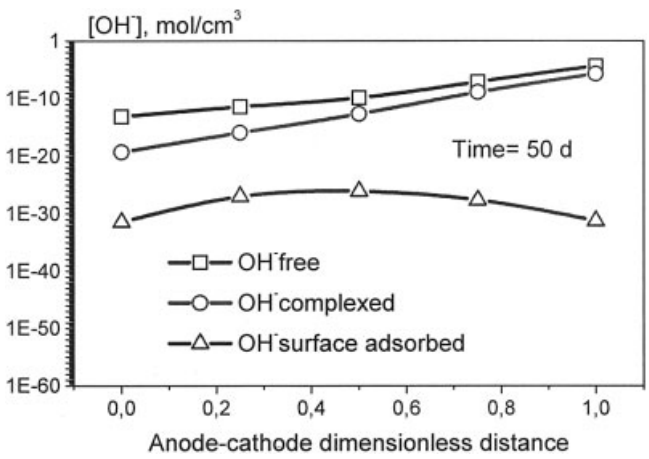

Figure 14. Hydroxyl speciation profiles at long time (50 d) for an electroremediation of a cadmium spiked kaolinite.

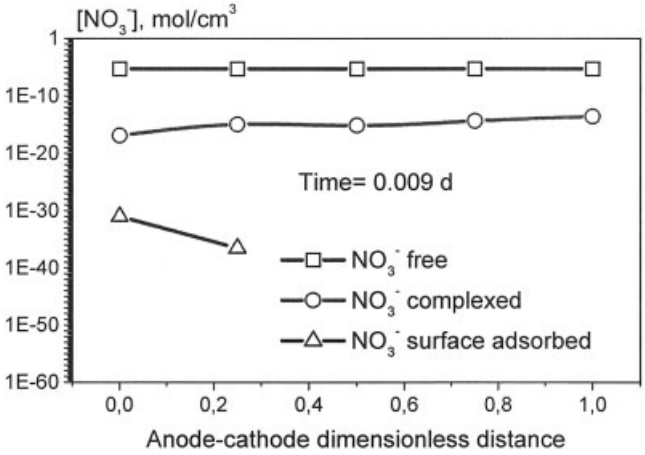

Figure 15. Nitrate speciation profiles at short time (0.009 d) for an electroremediation of a cadmium spiked kaolinite.

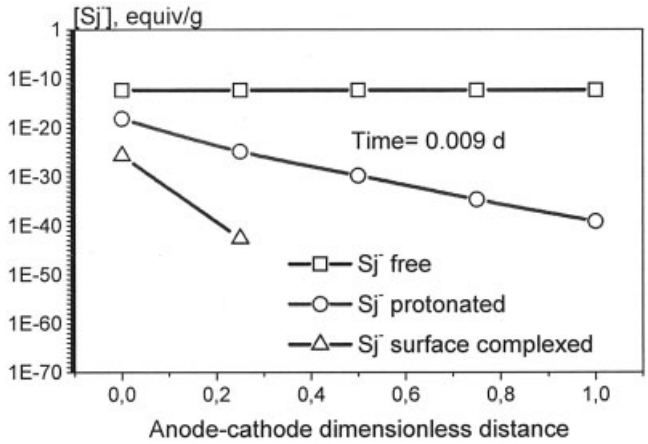

Figure 17. Soil sites speciation profiles at short time (0.009 d) for an electroremediation of a cadmium spiked kaolinite.

heavy metal polluted soil. This approach allowed demonstrating that soil surface sites are a key parameter that can not be neglected in the mathematical formulation.

Inclusion of Boltzmann's relationship to define soluble concentrations at the solid-fluid boundary, allowed for electric potential to be a driving force at the soil surface. Also, this inclusion allowed to smooth variations in velocity predictions.

Future work should be addressed to get experimental data of a cadmium-kaolinite system at different times; so far it is recommended to set up several experiments at identical conditions, and stop them at different times.

Notation

a_i = stoichiometric coefficient
a_{ik} = number of k ions required to form the i^{th} complexed species
c_i = i^{th} specie soluble concentration, mol cm^{-3}
c_{i0} = i^{th} specie bulk soluble concentration, mol cm^{-3}
c_{si} = surface adsorbed concentration of specie i, mol g^{-1}
c_α = α ionic species concentration, mol cm^{-3}
$c_{\alpha 0}$ = free α ionic species concentration, mol cm^{-3}
$c_{s\alpha}$ = α ionic species concentration on the solid phase, mol cm$^{-3}_{solid}$
c_m = membrane active sites concentration, mol g^{-1}
$c_{s\alpha,i}$ = surface adsorbed concentration of specie i, mol g^{-1}
e = unit electric charge, 1.609×10^{-20} C
k = Boltzmann's constant, 1.38×10^{-16} erg K^{-1}
k_{sm} = membrane hydraulic conductivity, cm s^{-1}
t = time, s
v = fluid velocity, cm s^{-1}
z_i = i^{th} specie electric charge, equiv mol^{-1}
z_m = membrane active sites charge, equiv mol^{-1}
B_k = k^{th} ionic species concentration in a soluble complex
D_i = i^{th} specie diffusion coefficient, cm^2 s^{-1}
F = Faraday's constant, 96489 C equiv^{-1}
I = electric current density, A cm^{-2}
K = ionic solution conductivity, S cm^{-1}
Kd_i = i^{th} ion exchange equilibrium constant
Ke_i = i^{th} complexed specie chemical equilibrium constant
N_i = i^{th} species ionic flux, mol cm^{-2} s^{-1}
P = hydrostatic pressure, dyne cm^{-2}
R = ideal gas constant, 8.314 J mol^{-1} K^{-1}
R_i = i^{th} species reaction rate term in aqueous phase, mol cm^{-3} s^{-1}
$R_{s\alpha}$ = α species reaction rate at the solid phase, mol cm^{-3} solid s^{-1}
Sj^- = soil surface sites, equiv g^{-1}
T = temperature, K

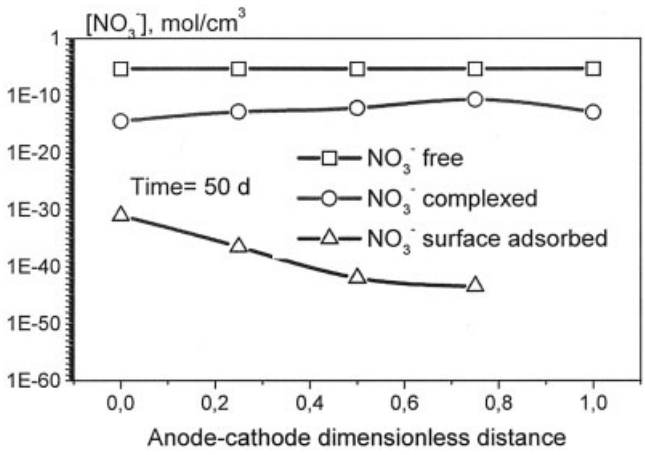

Figure 16. Nitrate speciation profiles at long time (50 d) for an electroremediation of a cadmium spiked kaolinite.

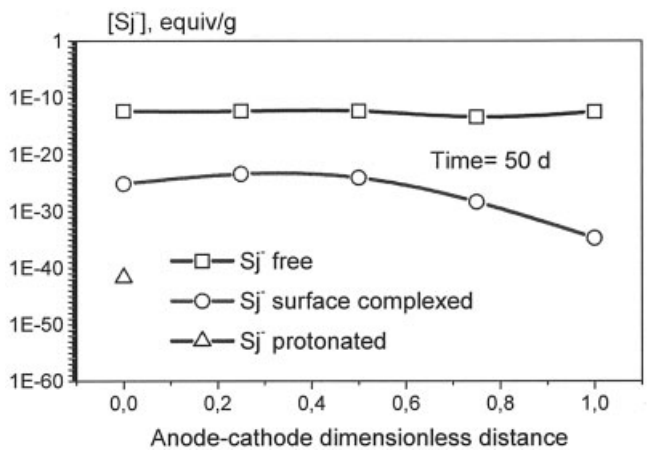

Figure 18. Soil sites speciation profiles at long time (50 d) for an electroremediation of a cadmium spiked kaolinite.

Greek Letters

χ_α = complexed α concentration, mol cm^{-3}
$\nu_{\alpha i}$ = stoichiometric coefficient
η = fluid viscosity, g cm^{-1} s^{-1}
θ = void ratio, cm^3 $_{\text{liquid}}$ cm^{-3} $_{\text{total}}$
Γ = solid phase electric conductivity, S cm^{-1}
Ψ = interface electric potential, V
Ψ_0 = bulk electric potential, V

Literature Cited

1. Hall JC, Raider R L, Graffton JA. EPA's *Heavy Metal Criteria.* Environment and Technology,1992, 260-263.
2. Naidu R, Kookana RS, Summer ME, Harter RD,Tiller KG. Cadmium sorption and transport in variable charge soils: A review. *J Environmental Quality*, 1997;26, 602-617.
3. Gunn AM, Winnard DA, Hunt DTE. *Trace Metal Speciation in Sediments and Soils*. In Kramer, J. and H. E. Allen, Metal Speciation: Theory, Analysis and Application. Lewis Publishers, Inc; 1988.
4. Pamucku S, Khan LI, Fang H-Y. Zinc detoxification of soils by electroosmosis. Transportation Research record 1288. TRB; 41–46.
5. Hicks, R. F., and Tondorff S. Electrorestoration of metal contaminated soils. *Environ Sci Technol*. 1994,28,2203-2210.
6. Hamed JT, Acar YB, Gale RJ. Pb(II) removal from kaolinite by electrokinetics. *J Geotechnical Eng.* 1991,117,241-271.
7. AcarYB. Hamed JT, Alshawabkeh AN. Gale RJ. Removal of cadmium (II) from saturated kaolinite by the application of electrical current. *Geotechnique*. 1994;44:229-254.
8. Pamucku, S., Wittle J. K. Electrokinetic removal of selected heavy metals from soil. *J Environ Progress*. 1992;11:241-250.
9. Cabrera-Guzmán, D., Swartzbaugh J. T. and Weissman A. The use of electrokinetics for hazardous waste site remediation. *J Air Waste Management Association*. 1990;40:1670-1676.
10. Lageman R. Pool W., and Sefinga G. Electroreclamation: theory and practice. *Chemistry and Industry*; 1989;18 Sept:585-590.
11. Hammet R. *A Study of the Process Involved in Electroremediation of Contaminated Soils. M. Sc Thesis*. University of Manchester, U.K. 1980.
12. Khan LI, Alam MS. Heavy metal removal from soil by coupled electric-hydraulic gradient. *J Environ Eng*. 1994;120:1524-1542.
13. Reed BR, Berg MT, Thompson JC, Hatfield JH. Chemical conditioning of electrode reservoirs during electrokinetic soil flushing of Pb-contaminated silt loam. J Environ Eng. 1995;121:805-815.
14. Yeung AT, Hsu Ch, Menom RJ. EDTA enhanced electrokinetic extraction of lead. J Geotechnical Eng. 1996;122:666-673.
15. Cox Ch D, Shoesmith MA, Ghosh MM. Electrokinetic remediation of mercury contaminated soils using Iodine/Iodide lixiviant. *J Environ Sci and Technol*. 1996;30:1933-1938.
16. ColettaTF, Bruell CJ, Ryan DK, Inyang HI. Cation-enhanced removal of lead from kaolinite by electrokinetics. *J Environ Eng*. 1997;123: 1227-1233.
17. Li Zh,Yu J-W, Neretnieks I. Electroremediation: removal of heavy metals from soils by using a cation selective membrane. *J Environ Sci and Technol*. 1998;32:394-397.
18. Baraud F, Tellier S, Astruc M. Ion velocity in soil solution during electrokinetic remediation. *J Hazardous Materials*. 1997;56:315-332.
19. Hamed JT, Badhra A. Influence of current density and pH on electrokinetics. *J Hazardous Materials*. 1997;55:279-294.
20. Baraud F, Tellier S, Astruc M. Temperature effect on ionic transport during soil electrokinetic treatment at constant pH. *J Hazardous Materials;* 1999;B64:263-281.
21. Chen J-L, Al-Abed SR. Cation transport and partitioning during a field test of electroosmosis. *Water Resources Research.* 1999;35:3841-3851.
22. Dzenitis JM. Soil chemistry effects and flow prediction in electroremediation of soil. *J Environ Sci and Technol*. 1997;31:1191-1197.
23. Acar YB, Gale RJ, Putnam GA, Hamed J, Wong RL. Electrochemical processing of soils: theory of pH gradient development by diffusion, migration and linear convection. *J Environ Sci Health.* 1990;A25 (6):687-714.
24. Acar YB, Alshawabkeh AN, Gale RJ. Fundamentals of extracting species from soils by electrokinetics. *J Waste Management*; 1993;13: 141-151.
25. Probstein RF, Hicks RE. Removal of contaminants from soils by electric fields. *Science.* 1993;260:498-503.
26. Shapiro AP, Probstein RF. Removal of contaminants from saturated clay by electroosmosis. *J Environ Sci and Technol*. 1993;27:283-291.
27. Jacobs RA, Sengun MZ, Hicks RE, Probstein RF. Model and experiments on soil electroremediation by electric fields. *J Environ Sci Health.* 1994;A29(9):1933-1955.
28. Alshawabkeh AN, Acar YB. Removal of contaminants from soils by electrokinetics: a theoretical treatise. *J Environ Sci Health*. 1992; A27(7):1835-1861.
29. Alshawabkeh AN, Acar YB. Electrokinetic remediation II: theoretical model. *J Geotechnical Eng*. 1996;122:186-196.
30. Jacobs Cardozo RA. *Two-Dimensional Modeling of the Removal of Contaminants from Soils by Electric Fields.* Massachusetts Institute of Technology;1995. PhD Thesis.
31. Teutli-León MM, Oropeza Guzmán MT, González I. Mathematical modeling of electrochemical remediation for soils under galvanostatic conditions. *J Environ Technol*. 2001;21:17-26.
32. Dzombak DA, Hudson RJM. Ion exchange. The contributions of diffuse layer sorption and surface complexation. In Huang Chin Pao Ch. R. O'Melia, *Aquatic Chemistry: Interfacial and Interspecies Processes.* J. Morgan, editor. American Chemical Society. 1995.
33. Hall PL. Clays: their significance, properties, origins and uses. In Wilson MJ. *A Handbook of Determinative Methods in Clay Mineralogy*, New York: Chapman and Hall; 1984.
34. Huang CP, Hsieh YS, Park SW, Ozden Corapcioglu M. Chemical interactions between heavy metal ions and hydrous solids. In James W. Paterson, James W, Roberto Passino. *Metal Speciation, Separation, and Recovery*. Lewis Publisher;1987.
35. Yeh GT, Tripathi VS. A critical evaluation of recent developments in hydrogeochemical transport models of reactive multicomponents. *Water Resources Research*. 1989;25:93-108.
36. Guymonn GL. Unsaturated zone hydrology. Chapters 2, 3, 4. Prentice Hall, Inc; 1994.
37. Shang, JQ, Lo KY, Inculet II. Polarization and conduction of clay-water electrolyte systems. *J of Geotechnical Eng*. 1995;121:243-248.
38. Mitchell JK. Conduction phenomena: from theory to geotechnical practice. *Géotechnique*. 1991;41:299-340.
39. Verbrugge MW, Hill RF. Ion and solvent transport in ion-exchange membranes. I. A macrohomogeneous mathematical model. *J Electrochem Society*. 1990;137:886-893.
40. Bird RB, Stewart WE, Lightfoot EN. Transport phenomena. New York: Wiley; 2002;Chapter 19:582-605.
41. Newman JS. Electrochemical systems, Prentice Hall, Inc; 1991; Chapters 11:22
42. Lindsay WL. *Chemical Equilibria in Soils*. Wiley Interscience Publication, chapter 19; 1979.
43. Högfeldt E. Stability constants of metal ion complexes. Part A: Inorganic Ligands. I. U. P. A. C. Chemical Data Series, #21. Pergamon Press;1982.
44. Rand B, Melton IE. Particle interactions in aqueous kaolinite suspensions. I. Effect of pH and electrolyte upon the mode of particle interaction in homoionic sodium kaolinite suspensions. *J Colloid and Interface Sci*; 1977;60(2):308-320.
45. Stumm W. Chemistry of the solid water interface: processes at the mineral-water and particle-water interface in natural systems. Chapters 3, 4, and 5. New York: Wiley; 1992.
46. Mc Bride M. Features of chemisorption on aluminosilicates and oxides. In Environmental chemistry of soils. Oxford University Press; 1994;122-127.
47. Finlayson PA. Nonlinear analysis in chemical engineering. New York: McGraw-Hill; 1994;Section 4.9:113-126.

Appendix A

Aqueous complexation between cadmium (Cd^{+2}) and hydroxyl (OH^-) ions

$$Cd^{+2} + nOH^{-1} \leftrightarrow [Cd(OH)_n]^{2-n}$$

$$K_n = \frac{[Cd(OH)_n]^{2-n}}{[Cd^{+2}][OH^{-1}]^n}, \quad n = 1 \ldots 6 \quad \text{(A1)}$$

Table A1. Equilibrium Constants

Chemical Specie	Equilibrium Constant	Log (K)	Reference	Conditions
$[SiOH_2]^+$	K_{d1}	2.8	34	0.1 M NaCl
SiOH	K_{d2}	−6.8	34	0.1 M NaCl
$[AlOH_2]^+$	K_{d3}	−8.2	34	0.1 M NaCl
AlOH	K_{d4}	−9.4	34	0.1 M NaCl
$[CdOH]^+$	K_1	−10.10	42	—
$Cd(OH)_2$	K_2	−20.30	42	—
$[Cd(OH)_3]^{-1}$	K_3	−33.01	42	—
$[Cd(OH)_4]^{-2}$	K_4	−47.29	42	—
$[Cd(OH)_5]^{-3}$	K_5	−61.93	42	—
$[Cd(OH)_6]^{-4}$	K_6	−76.81	42	—
$[Cd(NO_3)]^{+1}$	K_9	0.46	42	—
$Cd(NO_3)_2$	K_{10}	0.17	42	—
$[Cd(NO_3)_3]^{-1}$	K_{11}	−0.85	42	—
$Cd(OH)_2 \downarrow$	K_{so}	−14.6	43	1 M $NaClO_4$
$[AlOCd]^+$	K_{SC1}	4.87	34	0.05 M
AlOCdOH	K_{SC2}	5.35	34	0.05 M
$[AlOCd(OH)_2]^{-1}$	K_{SC3}	5.38	34	0.05 M
$(SiO)_2Cd$	K_{SC4}	0.66	34	0.1 M $NaNO_3$
$(SiO)_2CdOH$	K_{SC5}	5.6	34	0.1 M $NaNO_3$
$[SiOCd(OH)_2]^{-1}$	K_{SC6}	6.69	34	0.1 M $NaNO_3$
$AlOH_2(NO_3)$	K_{SC7}	6.9	44	0.1 M $NaNO_3$
$SiOH_2(NO_3)$	K_{SC8}	6.9	44	0.1 M $NaNO_3$

Aqueous complexation between cadmium (Cd^{+2}) and nitrate (NO_3^-) ions

$$Cd^{+2} + mNO_3^- \leftrightarrow [Cd(NO_3)_m]^{2-m}$$

$$K_m = \frac{[Cd(NO_3)_m]^{2-m}}{[Cd^{+2}][NO_3^{-1}]^m}, \quad m = 1 \ldots 3 \qquad \text{(A2)}$$

Cadmium precipitation as solid cadmium hydroxide

$$Cd(OH)_2 \downarrow \leftrightarrow Cd^{+2} + 2OH^{-1} \quad K_{so} = [Cd^{+2}][OH^{-1}]^2 \qquad \text{(A3)}$$

Soil sites surface reactions

$$SiOH_2^+ \leftrightarrow SiOH + H^+ \quad K_{d1} = \frac{[SiOH]_s[H^+]}{[SiOH_2^+]_s} \qquad \text{(A4)}$$

$$SiOH \leftrightarrow SiO^- + H^+ \quad K_{d2} = \frac{[SiO^-]_s[H^+]}{[SiOH]_s} \qquad \text{(A5)}$$

$$AlOH_2^+ \leftrightarrow AlOH + H^+ \quad K_{d3} = \frac{[AlOH]_s[H^+]}{[AlOH_2^+]_s} \qquad \text{(A6)}$$

$$AlOH \leftrightarrow AlO^- + H^+ \quad K_{d4} = \frac{[AlO^-]_s[H^+]}{[AlOH]_s} \qquad \text{(A7)}$$

Surface reactions onto aluminol (AlO^-) sites

$$Cd^{+2} + AlO^-(s) = [AlO(Cd)]^+(s) \quad K_{SC1} = \frac{\lfloor (AlOCd)^+ \rfloor_s}{[Cd^{+2}][AlO^-]_s} \qquad \text{(A8)}$$

$$[CdOH]^+ + AlO^-(s) = [AlO(CdOH)](s) \quad K_{SC2} = \frac{[AlO(CdOH)]_s}{[CdOH)^+][AlO^-]_s} \qquad \text{(A9)}$$

$$[Cd(OH)_2] + AlO^-(s) = [AlO(Cd(OH)_2)](s) \quad K_{SC3} = \frac{[AlO(Cd(OH)_2)]_s}{[Cd(OH)_2][AlO^-]_s} \qquad \text{(A10)}$$

Surface reactions onto silanol (SiO^-) sites

$$Cd^{+2} + 2SiO^-(s) = [(SiO)_2Cd](s) \quad K_{SC4} = \frac{[(SiO)_2Cd]_s}{[Cd^{+2}][SiO]_s^2} \qquad \text{(A11)}$$

$$[CdOH]^{+1} + 2SiO^-(s) = [(SiO)_2Cd(OH)]^{-1}(s) \quad K_{SC5} = \frac{[(SiO)_2Cd(OH)]_s}{[CdOH][SiO^-]_s^2} \qquad \text{(A12)}$$

$$[Cd(OH)_2] + 2SiO^-(s) = [(SiO)_2Cd(OH)_2]^{-2}(s) \quad K_{SC6} = \frac{[(SiO)Cd(OH)_2]_s}{[Cd(OH)_2][SiO]_s^2} \qquad \text{(A13)}$$

$$NO_3^{-1} + [(AlO)H_2]^{+1}(s) = [(AlO)H_2(NO_3)]^0(s) \quad K_{SC7} = \frac{[(AlO)H_2(NO_3)]_s}{[NO_3][(AlO)H_2]_s} \qquad \text{(A14)}$$

$$NO_3^{-1} + [(SiO)H_2]^{+1}(s) = [(SiO)H_2(NO_3)]^0(s) \quad K_{SC8} = \frac{[(SiO)H_2(NO_3)]_s}{[(SiO)H_2]_s[NO_3]} \qquad \text{(A15)}$$

Manuscript received Jun. 28, 2004, and revision received Oct. 12, 2004.